Since January 2020 Elsevier has created a COVID-19 resource centre with free information in English and Mandarin on the novel coronavirus COVID-19. The COVID-19 resource centre is hosted on Elsevier Connect, the company's public news and information website.

Journal of Photochemistry & Photobiology, B: Biology 240 (2023) 112667

Contents lists available at ScienceDirect

Journal of Photochemistry & Photobiology, B: Biology

journal homepage: www.elsevier.com/locate/jphotobiol

Affinity binding of COVID-19 drug candidates (chloroquine/hydroxychloroquine) and serum albumin: Based on photochemistry and molecular docking

Lan-Yi Hu, Ye Yuan, Zi-Xuan Wen, Yi-Yue Hu, Miao-Miao Yin *, Yan-Jun Hu *

Hubei Key Laboratory of Pollutant Analysis & Reuse Technology, College of Chemistry and Chemical Engineering, Hubei Normal University, Huangshi 435002, PR China

ARTICLE INFO

Keywords:
COVID-19
Chloroquine
Hydroxychloroquine
Serum albumin
Photochemistry
Molecular docking

ABSTRACT

Chloroquine (CQ) and hydroxychloroquine (HCQ) show good efficacy in the treatment of SARS-CoV-2 in the early stage, while they are no longer recommended due to their side effects. As an important drug delivery carrier, serum albumin (SA) is closely related to the efficacy of drugs. Here, the affinity behaviour of chloroquine and hydroxychloroquine with two SA were investigated through the multispectral method of biochemistry and computer simulation. The results showed that the intrinsic emission of both SA was quenched by CQ and HCQ in a spontaneous exothermic entropy reduction static process, which relied mainly on hydrogen bonding and van der Waals forces. The lower binding constants suggested weak binding between the two drugs and SA, which might lead to differences in efficacy and possibly even to varying side effects. Binding site recognition demonstrated that CQ preferred to bind to the two sites of both SA, while HCQ tended to bind to site I of SA. The results of conformational studies demonstrated that CQ and HCQ could affect the structure of both SA by slightly increasing the α-helix content of SA. Finally, we combine the results from experimental start with molecular simulations to suggest drug modifications to guide the design of drugs. This work has important implications for guiding drug design improvements to select CQ derivatives with fewer side effects for the treatment of COVID-19.

1. Introduction

So far in 2019, severe acute respiratory syndrome (SARS-CoV-2) induced “Coronavirus Disease 2019” (COVID-19) has severely impacted most countries' public health and regional economies worldwide [1]. The novel coronavirus and its mutant strains have more than 300 million cumulative infections worldwide and possess a high lethality rate [2,3]. Due to the novel coronavirus's variability and complex clinical symptoms, it is impossible to find clinical treatments and develop specific drugs quickly [4,5]. Therefore, the primary treatment method is choosing available antiviral drugs in clinical medicine.

In early clinical treatment, remdesivir, lopinavir/ritonavir, arbidol, ribavirin, chloroquine (CQ) and hydroxychloroquine (HCQ) have demonstrated therapeutic efficacy in patients with COVID-19. They can rapidly turn negative by reducing the viral load in the patient through different routes [6]. Among them, CQ and HCQ have excellent clinical and pathological results in patients with COVID-19. Therefore, they were urgently approved by the US Food Safety Administration in 2020 as drugs for the treatment of COVID-19 [7,8]. Chloroquine and hydroxychloroquine are derivatives of quinoline and have been used for 70 years for many different types of autoimmune diseases because of their excellent broad-spectrum antiviral activity [9]. Therefore, some researchers have suggested that quinolines, which are structurally similar to chloroquine drugs, are potential COVID-19 therapeutic agents, and they have used computer simulation techniques to suggest that some quinoline derivatives such as saquinavir, elvitegravir, etc. may be effective COVID-19 inhibitors [10]. The structure of CQ and HCQ are shown in Fig. 1. The only structural difference between them is an additional -OH group at the end of the HCQ branched chain, which made HCQ more effective than CQ in treatment [11]. Related studies have shown that CQ/HCQ interferes with the glycosylation process of ACE2 protein to block the association of SARS-CoV-2 with receptors on the membrane, thereby suppressing in vitro replication of SARS-CoV-2 [12,13]. Clinical trials point to potential safety problems with the long-term use of CQ/HCQ, such as increase in the risk of diarrhoea and nausea/vomiting in patients, and may further lead to hypovolemia disorders, hypotension and acute kidney injury [13,14]. Many experiments have shown that the use of CQ and HCQ leads to a prolongation of

* Corresponding authors.
E-mail addresses: yinmm@hbnu.edu.cn (M.-M. Yin), huyj@hbnu.edu.cn (Y.-J. Hu).

https://doi.org/10.1016/j.jphotobiol.2023.112667
Received 8 December 2022; Received in revised form 16 January 2023; Accepted 30 January 2023
Available online 2 February 2023
1011-1344/

the post-correction ventricular systolic interval (QTc) in patients, QTc during treatment is a simple risk indicator of death that reflects the state of myocardial inflammation in patients with COVID-19[15]. QTc prolongation may be related to the blood concentration of drugs in patients [16]. Therefore, research and refinement of chloroquine drugs are highly necessary.

As one of the essential plasma proteins in living organisms, serum albumin (SA) is involved in regulating acid-base balance and catalyzing metabolic reactions and is an indispensable transporter and drug-binding protein in the body [17,18]. Human serum albumin (HSA), which accounts for approximately 60% of human plasma proteins, is a carrier of exogenous and endogenous drug small molecules in humans [19,20]. Bovine serum albumin (BSA) has high homology with HSA and is often used to compare with HSA [21,22].

It is inevitable that CQ and HCQ drugs will come into contact with SA during transport in the organism. Additionally, as a common transport protein, SA plays an essential part in the transport of drugs to their site of action, and some extent related to the efficacy of the drug [23,24]. Therefore, it is essential to study the affinity interaction between chloroquine and hydroxychloroquine with SA [25]. In this work, we explored the affinity binding behaviour of CQ and HCQ with SA. Using variety of techniques including steady-state fluorescence, UV–vis spectroscopy transient fluorescence spectroscopy, circular dichroism (CD) spectroscopy and Fourier transform infrared (FT-IR) spectroscopy were used to study the interaction mechanisms, intensity, site, main forces and structural changes of SA.

2. Materials and Experiments

2.1. Materials

CQ and HCQ were purchased from Aladdin and dissolved in ultrapure water. Warfarin (War), Ibuprofen (Ibu), BSA and HSA were purchased from Sigma-Aldrich. SA were dissolved in phosphate-buffered saline (PBS) buffer with pH = 7.40. Analytical purity of all chemicals and components were used in experiments.

2.2. Experiments

2.2.1. UV–vis Spectroscopy

UV–vis spectroscopy experiments were conducted with UV-9000 spectrophotometer from Source West, Shanghai, China. The recording range was set as 220 nm to 400 nm with PBS solution as background. The final concentration of SA was made to be 10.00 μM, and the concentrations of CQ/HCQ were from 0.00 μM to 40.00 μM. CQ/HCQ were added to the sample cell at 25 °C, stirred for 30 s and stood for 1 min, and then the absorption spectra were scanned.

2.2.2. Fluorescence Spectroscopy

Fluorescence spectroscopy experiments were performed with LS-55 spectrometer from Perkin Elmer, USA. The Ex wavelength was 280 nm, and each curve was the average of three consecutive scans. In the binding site recognition experiments, the concentrations of War and Ibu were kept consistent with those of SA. In the synchronous fluorescence spectroscopy experiments, the wavelength difference ($\Delta\lambda$) was chosen to be 60 nm or 15 nm, and scan range was set as 220 nm to 500 nm. In the above three fluorescence experiments, the final concentrations of SA were made to be 10.00 μM, and the concentrations of CQ/HCQ were from 0.00 μM to 40.00 μM. CQ/HCQ were added to the sample cell at 25 °C and then stirred for 30 s. After stabilization for 1 min, the spectra were scanned. In the experiments of 3D fluorescence, the emission range was set as 195 nm to 550 nm, the excitation range was set as 195 nm to 450 nm and acquisition interval was set as 3 nm. The experiments were designed with a final concentrations of 5.00 μM for both SA and CQ/HCQ, and each group was deducted against the background of the three-dimensional fluorescence pattern of CQ/HCQ in PBS. The FS5 steady-state FL fluorescence spectrometer (Edinburgh, UK) was used to measure the fluorescence lifetime of SA in the absence and presence of CQ/HCQ. 260 nm EPLD light source was selected as the light source and the excitation wavelength and emission wavelength were set as 280 nm and 347 nm, respectively. The final concentrations of SA and CQ/HCQ were made to be 10.00 μM, and after scanning the fluorescence lifetime curve of pure SA, CQ/HCQ were added to the original solution and then stirred for 30 s to stabilize for 2 min before scanning.

2.2.3. FT-IR Spectroscopy

FT-IR spectroscopy was performed with Thermo Nicolet iS5 iD1 spectrophotometer. The test scope was setas 1750 cm^{-1} to 1500 cm^{-1} and the spectral resolution was set as 2 cm^{-1}. Fourier deconvolution and second-order derivatives were done using pikefit-v4.12. The concentration of SA used in the experiment was 500.00 μM, and make the concentration of CQ/HCQ added to the system with SA was 1: 1. The SA used in the experiment was mixed with CQ/HCQ at 25 °C and incubated for 30 min before use.

2.2.4. CD Spectroscopy

CD spectroscopy was performed with Applied Photo-205 physics Limited at 25 °C. The cuvette optical path used was 0.1 cm and the range of scanning was set as 200 nm to 330 nm with a pitch of 0.5 nm. The final concentration of SA was 5.00 μM and the concentration gradient of CQ/HCQ were both set as 5.00 μM, 15.00 μM and 30.00 μM.

2.2.5. Computer Simulation Combination

The computer simulation software used for the simulations was SYBYL-X 2.1.1 (Tripos, USA). The three-dimensional spatial structure of SA was downloaded from the protein database from the RSCB, PDB (Protein Data Bank) numbers 4OR0 and 1H9Z. Pymol open source version was used for visual analysis.

3. Results and Discussion

3.1. Fluorescence Quenching Mechanism

As a sensitive and straightforward method, steady state fluorescence has been extensively applied to the analysis of drug-biomacromolecule interactions [26]. Due to the existence of tryptophan (Try) and

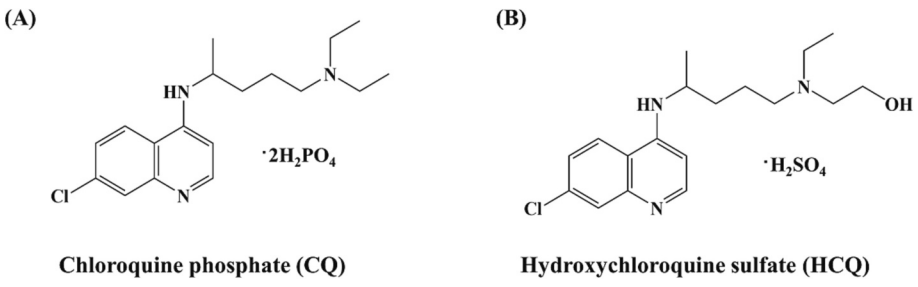

Chloroquine phosphate (CQ) Hydroxychloroquine sulfate (HCQ)

Fig. 1. Molecular plane structural formula of CQ (A) and HCQ (B).

tyrosine (Tyr), SA exhibits intrinsic fluorescence that can be used for research [27]. As shown in Fig. 2, both CQ and HCQ could regularly quench the fluorescence of SA, indicating that there were interactions between both drugs and SA. With the increasing concentration of CQ and HCQ, the emission peak position of both serum proteins had a red-shift, indicating that CQ and HCQ could affect the polarity of the microenvironment of Try and Tyr. An isoemission point appeared near 389 nm, in which the concentration of bound and free drugs in the solution reached a balance.

Fluorescence quenching mechanism is normally classified into two modes: namely static mode and dynamic mode. To further study the quenching mechanism of CQ and HCQ to the emission of serum proteins, we studied the influence of two drugs on the fluorescence lifetime of SA. Normally, the fluorescence lifetime of fluorophores during dynamic quenching will decrease with the addition of quenching agent, while in the static quenching process, it is not affected by the quenching agent [28]. The fluorescence lifetime was calculated with Eq. (1):

$$\tau = \tau_1 A_1 + \tau_2 A_2 \quad (1)$$

where τ_1 and τ_2 were the decay time, A_1 and A_2 were the pre-exponential factors; these parameters are listed in Table S1. As shown in Fig. 3, with the addition of CQ and HCQ, the fluorescence lifetime of the two serum proteins were not obviously changed, suggesting that the fluorescence quenching mechanism of CQ and HCQ to the two SA were both in static mode. The minor change in fluorescence lifetime might arise from the energy transfer [29].

We conducted UV–vis absorption spectroscopy experiments to verify above results. The Tyr and Try of SA could cause significant absorption at 222 nm and 280 nm owing to π-π* and n-π* transitions [30]. In general, the dynamic quenching mechanism will not affect the excited state of fluorescent group and has no obvious effect on the absorption spectrum. Conversely, the complex produced by the static quenching will cause significant perturbation of the spectrum of the fluorescent group [31]. As shown in Fig. S1, the peaks around 252 nm and 345 nm were absorption of CQ and HCQ itself (red dotted line in Fig. S1), and with the addition of CQ and HCQ, the characteristic absorptions of the two SA at 280 nm were significantly enhanced, further indicating that there were interactions between the two drugs and SA. We subtracted the absorption value of the drugs from that of the SA-drug complexes at 280 nm, and found that they were not equal to the absorption value of SA (insets of Fig. S1) indicating that the quenching mechanism of two drugs to the emission of SA were both in static mode.

The change rules of the quenching constants between drugs and proteins at different temperatures are often used to judge the quenching mechanism. Generally, dynamic quenching is induced by intermolecular collision, and the probability of collision at high temperatures will increase, resulting in the increase of quenching constant. On the contrary, in static mode, a ground state complex will be formed between the quenching agent and the fluorescent group, and high temperature will reduce the stability of the complex, thus reducing the quenching constant [32]. The quenching constants were calculated with classical Stern-Volmer equation (Eq. (2)) [33]:

$$\frac{F_0}{F} = 1 + K_{SV}[Q] \quad (2)$$

where F_0 and F were the fluorescence intensity of SA in the absence and presence of drugs, respectively. [Q] represented the concentration of the drug. K_{SV} represented the quenching constant. The quenching constants of CQ and HCQ to the emission of SA were listed in Table S2. The order of magnitude of K_{SV} were both in the third power of ten, indicating that the interactions between the two drugs and SA were very weak. With the increasing temperature, the quenching constants of both drugs to SA decreased, indicating that the quenching mechanisms of CQ and HCQ to SA were both in static mode, which was consistent with the conclusions above.

3.2. Binding Intensity, Site and Main Forces

Binding constants are often used to measure the binding capacity between drugs and biomacromolecules. For obtaining the bonding

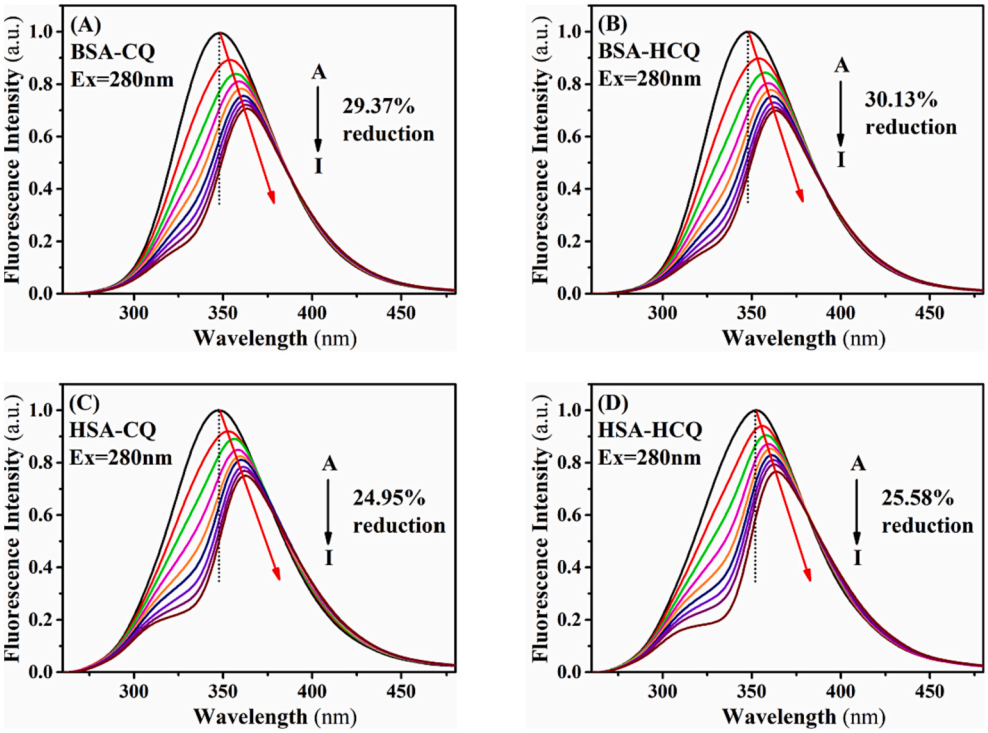

Fig. 2. Fluorescence emission spectra of BSA at different concentrations of CQ (A) and HCQ (B); Fluorescence emission spectra of HSA at different concentrations of CQ (C) and HCQ (D). The concentrations of SA were 10.00 μM and the final concentrations of CQ and HCQ were both 40.00 μM.

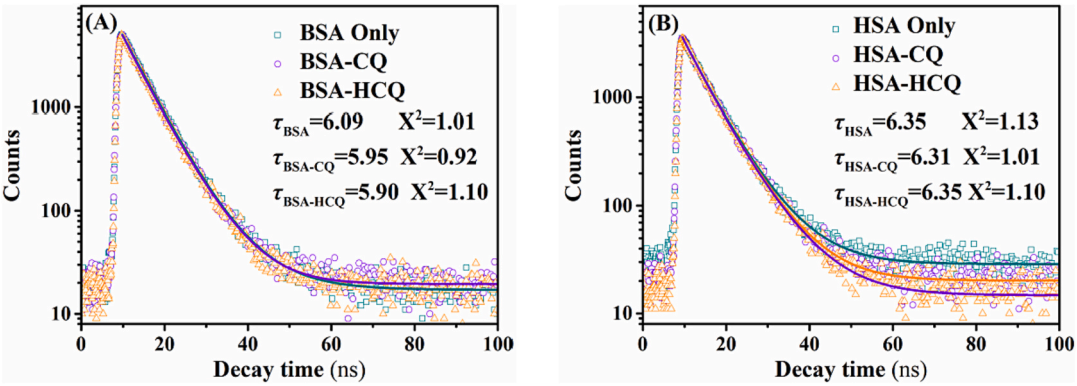

Fig. 3. (A) Fluorescence lifetime fitting curve of BSA in the absence and presence of CQ and HCQ; (B) Fluorescence lifetime fitting curve of HSA in the absence and presence of CQ and HCQ.

strength of CQ and HCQ to SA, the emission quenching data were processed by double logarithmic (Eq. (3)) [34]:

$$log\left(\frac{F_0 - F}{F}\right) = logK_b + nlog[Q] \quad (3)$$

where F_0 and F were the same as Eq. (2). n represented the combined proportion and K_b represented binding constant. The binding constants of CQ and HCQ to the two kinds of SA were listed in Table S3. From the value of K_b, the binding capacity of the two drugs with BSA were greater than that with HSA, and the binding capacity to SA of HCQ was stronger than that of CQ. The order of magnitude of K_b were both in the second power of ten, which once again indicated that the interactions between the two drugs and SA were very weak. It is well known that the binding capacity is an essential parameter that should be considered in pharmacokinetics. Generally, drugs with low binding rates tend to be released early or metabolized more quickly, while drugs with high binding rates are not easily metabolized and excreted, both of which may have side effects on the body [35]. Pharmacokinetic studies of CQ/HCQ in the literature showed that they were mainly bound to plasma albumin with a binding rate of 50% ~ 60%, and they were widely distributed in the tissues of the human body [36]. The binding constants we obtained confirmed that the binding between CQ and HCQ to SA were very weak, which might lead to releasing in advance and causing negative impact on the human body. Meanwhile, we believe that the difference in the binding capacity of these two drugs may affect the efficacy of the drugs and even exhibit different side effects.

It has been documented that drug molecules ~~are~~ mainly bind to the hydrophobic cavity of serum albumin, with the central regions locate at sub-structural domains IIA (Site I) and IIIA (Site II) [37]. Hence, we used classical site probes, namely warfarin and ibuprofen, which could label site I and site II, respectively, to perform fluorescence competition experiments and determine the specific binding sites of CQ and HCQ to SA. The quenching constants of both drugs to the emission of SA in the absence and presence of warfarin and ibuprofen were still obtained by fitting the data with Eq. (2) and were listed in Table S4. For CQ, with the addition of Ibu and War, the quenching constants decreased to some extent, indicating that CQ tended to bind to the two sites of SA, and bond more strongly to site I. For HCQ, the quenching constants significantly decreased with the addition of War, which suggested that HCQ was mainly bound to the site I of SA. Molecular docking has also been used as a common approach to investigate the binding sites between drug molecules and biomacromolecules [38]. In order to further study the binding sites between the two drugs and SA, we conducted molecular docking experiments and the results were shown in Fig. 4 and Table S5. CQ and HCQ docked with amino acids in the 4 Å range in site I and site II of both SA after semi-flexible docking in a simulated physiological environment (Fig. 4). From the results of scoring function (Table S5), CQ

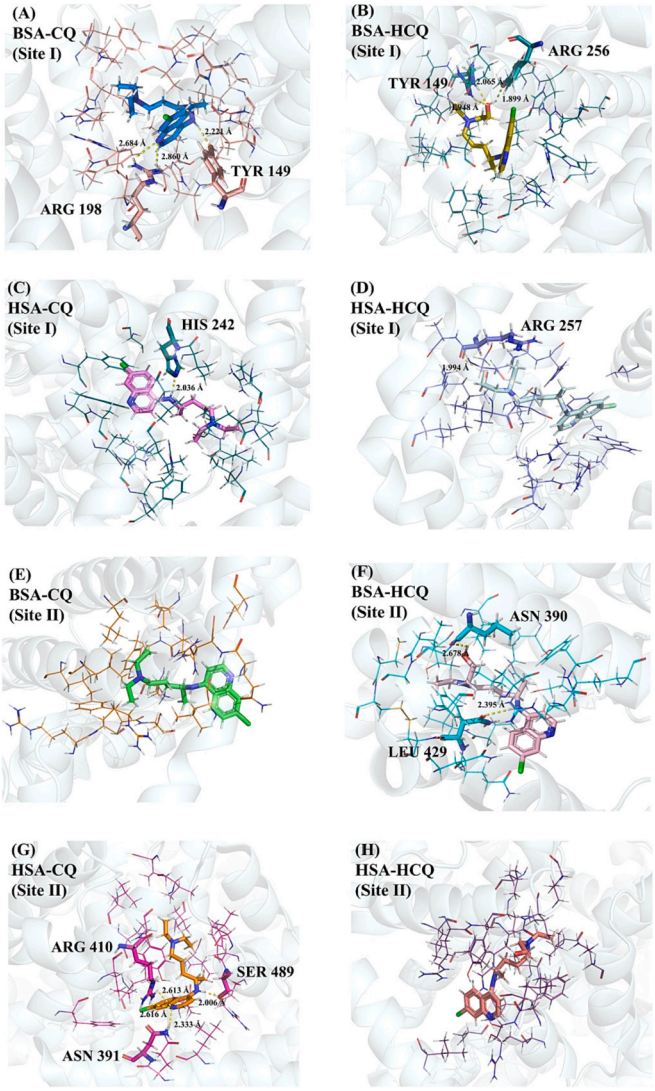

Fig. 4. Molecular docking of CQ and HCQ to the site I and site II of SA in 3D conformation within 6 Å. CQ (A) and HCQ (B) to the site I of BSA; CQ (C) and HCQ (D) to the site I of HSA; CQ (E) and HCQ (F) to the site II of BSA; CQ (G) and HCQ (H) to the site II of HSA.

tended to bind to the two sites of BSA, while HCQ tended to bond to the site I of BSA. With respect to HSA, CQ tended to bind to the site II, while HCQ tended to bond to the site I. Based on the results of experiments and

theoretical calculations, we found that CQ tended to bond to the two sites of SA, and HCQ tended to bond to the site I of SA.

The amino acid sequences of BSA and HSA have 76% identity and 88% similarity, showing high homology. Therefore, researchers can predict the binding behaviour of drugs and HSA from that of BSA [22]. However, some studies have shown that the same drugs may have different binding behaviours to BSA and HSA [39]. In this work, we also found that in the interactions between two drugs and SA, there were small differences between the two SA, such as binding capacity, which might be related to the different amino acid sequences of the hydrophobic binding cavities of BSA and HSA [40]. We compared the possible conformation of CQ and HCQ in the two sites of SA with molecular simulations. It demonstrated that CQ and HCQ could exhibit a more flexible folding conformation in the binding cavity of BSA, while showed a fixed linear conformation when bound to HSA (Fig. 5). Hence, we believed that the hydrophobic cavity of BSA was more suitable for insertion and binding of CQ and HCQ than HSA, which could be a reason for the difference in drug binding behaviour.

Thermodynamic parameters play important roles in judging the interaction direction and main forces between drugs and biomacromolecules. To obtain the direction and thermal effect of the interactions between two drugs and SA, we calculated the thermodynamic parameters depending on the binding constants at various temperatures obtained above with Eqs. (4) and (5) and listed in Table 1 [41]:

$$lnK_b = -\frac{\Delta H}{RT} + \frac{\Delta S}{R} \tag{4}$$

$$\Delta G = \Delta H - T\Delta S \tag{5}$$

where ΔH, ΔG, and ΔS represented the change values of enthalpy, Gibbs free energy and entropy, respectively. The values of ΔG, ΔH and ΔS were all less than zero, indicating that the interactions between two drugs and SA were both spontaneous with exothermic and entropy reduction processes. From the absolute values of ΔH, we found those of HCQ were larger than CQ, indicating that it emitted more heat in the interactions between HCQ and SA, which might be related to the stronger interactions between HCQ and SA than CQ (Table S3).

Binding forces between drugs and biomacromolecules are divided into four main types: hydrogen bonding, electrostatic forces, hydrophobic forces and van der waals forces [28]. Based on the classical Ross theory, the ΔH and ΔS of the interactions between two drugs and SA were all less than zero, indicating that hydrogen bonding and van der Waals forces were the major forces of interaction [41]. We further verified whether there were hydrogen bonds between the two drugs and SA with molecular docking, and the hydrogen bonds between CQ and HCQ with amino acids in the 4 Å range at site I and site II of BSA and HSA were shown in Fig. 4 and Table S5. We found that CQ formed hydrogen bonds with TYR 149 (2.221 Å) and ARG 198 (2.684 Å and 2.860 Å) at site I (Fig. 4A), while failing to form hydrogen bonds at site II of BSA (Fig. 4E). In terms of HSA, CQ formed a hydrogen bond in the site I with HIS 242 (2.036 Å) (Fig. 4C) and four hydrogen bonds with ASN 391 (2.333 Å), ARG 410 (2.616 Å and 2.613 Å) and SER 489 (2.06 Å) in the site II (Fig. 4G). HCQ formed hydrogen bonds with TYR 149 (1.948 Å and 2.065 Å) and ARG 256 (1.899 Å) in Site I (Fig. 4B) and ASN 390 (2.678 Å) and LEU 429 (2.395 Å) in Site II of BSA (Fig. 4F). In terms of HSA, HCQ formed a hydrogen bond with ARG 257 (1.944 Å) in site I (Fig. 4D), while failing to form hydrogen bonds at site II (Fig. 4H). Overall, the main forces of the interactions between two drugs and SA were hydrogen bonds and van der Waals forces.

3.3. Perturbation of SA Structure

The structure destruction will affect the physiological function of protein, so it is essential to elucidate the perturbation of drug on the structure of proteins. Synchronous fluorescence techniques enable to explore the effect of drugs on the polarity of the microenvironment of amino acid residues of proteins [42]. Generally, we can set $\Delta\lambda = 15$ nm or $\Delta\lambda = 60$ nm to study the influence of drugs on the polarity of the surrounding environment of Tyr and Try residues, respectively. Results shown in Fig. S2, both drugs made the emission peak position of Try residues have varying degrees (4.5–6.0 nm) red-shift for both SA (Fig. S2-D), indicating that CQ and HCQ could enhance the polarity and

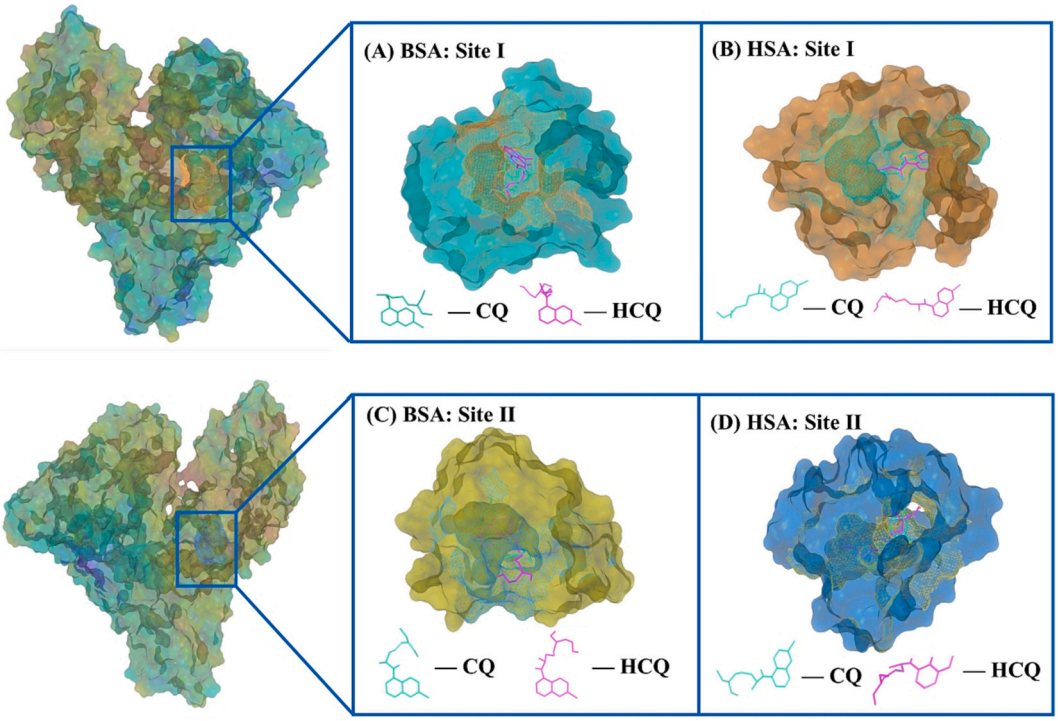

Fig. 5. Possible conformations of CQ and HCQ binding to the site I of BSA (A) and HSA (B); Possible conformations of CQ and HCQ binding to the site II of BSA (C) and HSA (D);

Table 1
Thermodynamic parameters of the interactions between two drugs and SA at 298 K, 304 K and 310 K.

System	BSA				HSA		
	T (K)	ΔH (kJ·mol^{-1})	ΔG (kJ·mol^{-1})	ΔS (J·mol^{-1}·K^{-1})	ΔH (kJ·mol^{-1})	ΔG (kJ·mol^{-1})	ΔS (J·mol^{-1}·K^{-1})
	298		−13.58			−11.60	
CQ	304	−25.98	−13.33	−41.62	−44.54	−10.94	−110.56
	310		−13.08			−10.27	
	298		−14.41			−13.49	
HCQ	304	−36.27	−13.97	−73.35	−64.33	−12.47	−170.62
	310		−13.53			−11.44	

weak the hydrophobicity of the surrounding environment of Try residues for both SA. On the contrary, they made a slight blue-shift in emission peaks of Tyr residue (Fig. S2-H), indicating that both drugs could reduce the polarity and increase the hydrophobicity of the microenvironment of Tyr residues for both SA. As shown in Fig. S3, the peaks at 325 nm ($\Delta\lambda = 60$ nm) and 345 nm ($\Delta\lambda = 15$ nm) were derived from the emission of CQ and HCQ itself. We found that the addition of SA also made the emission peak positions of CQ and HCQ shift to a certain extent (Fig. S2) indicating that SA also changed the polarity of the environment around drugs, that was, the drug-protein action process is a mutual influence process.

CD spectroscopy can be used as an accurate method for examining the structure effect of drugs on proteins. Owing to n-π* transition of α-helix, both SA have two characteristic downward peaks at around 208 nm and 222 nm in CD spectral curve [43]. The main second-order structure of the protein is α-helix, which can be calculated with Eqs. (6) and (7) [34]:

$$\alpha - \text{helix}(\%) = \frac{(-\text{MRE}_{208} - 4000)}{33000 - 4000} \times 100\% \quad (6)$$

$$\text{MRE}_{208} = \frac{\text{CD(mdeg)}}{10 \times nlC_P} \quad (7)$$

where MRE_{208} was the average residual ellipticity at 208 nm, and C_P was the molar concentration of protein. The path length was a value of 0.10 cm for l, and n was the number of amino acid residues. Through calculation, with the increasing concentrations of CQ and HCQ, the α-helix contents of the two SA were slightly increased (Fig. S4 and the signal peaks of SA at 208 and 222 nm had also moved slightly (Insets of Fig. S4 indicating that CQ and HCQ could slightly tight the structure of protein peptide chain [43]. Meanwhile, we found that HCQ increased the a-helix of both SA (BSA: 2.24%, HSA: 2.20%) slightly more than those of CQ (BSA: 1.63%, HSA: 1.52%), which might also be related to the stronger interactions between HCQ and SA than CQ (Table S3).

FT-IR spectroscopy is also usually used in investigating the effect of drugs on the structure of biomacromolecules [44]. As shown in Fig. 6, the FT-IR spectroscopy of both SA exhibited amide I band (C=O) between 1700 and 1600 cm^{-1} and amide II band (N-H and C-N) between 1550 and 1500 cm^{-1}. Both SA showed a significant change in amide I band with the addition of CQ and HCQ, indicating that the two drugs might affect the secondary structure of SA by influencing the amide I band. The specific content of the secondary structure of SA was obtained by fourier deconvolution and second derivative of the amide I band [45]. When CQ and HCQ were present, the content of α-helix in both SA were increased, which were converted from β-sheet or random coil (Fig. 7C-H), indicating that the architecture of SA became more compact and ordered, which was in accordance with the findings of CD.

3D fluorescence technique can directly observe the structural effects of drugs on proteins [46]. As shown in Fig. 7, peaks A and B were rayleigh scattering peaks of SA, the peak 1 ($E_x = 278$ nm) represented the fluorescence information of amino acid residues of SA, and the peak 2 ($E_x = 230$ nm) represented the information of polypeptide backbone structures of SA [46]. With the addition of CQ and HCQ, the intensity of peak 1 of BSA was reduced from 2143.0 nm to 1837.0 nm (CQ) and 1815.0 nm (HCQ), respectively, and that of HSA was reduced from 1658.0 nm to 1561.0 nm (CQ) and 1349.0 nm (HCQ), respectively. This phenomenon indicated that both drugs could effectively quench the intrinsic fluorescence of amino acid residues in SA, which was consistent with the previous conclusion. Additionally, Peak 2 of BSA was quenched from 676.3 nm to 481.6 nm and 482.2 nm, respectively, while peak 2 of HSA was quenched from 662.7 nm to 601.0 nm and 443.8 nm by CQ and HCQ, indicating that both drugs had effected on the protein skeleton of SA [47].

Overall, the results of conformational studies demonstrated that CQ and HCQ could affect the structure of both SA by increasing the α-helix content of SA. However, this effect was relatively weak, meaning that CQ and HCQ have less impact on the functionality of the protein.

3.4. Molecular Simulation of Other CQ Derivatives and SA

According to the above results, the additional hydroxyl group made it exhibited a greater binding ability and structural influence with SA, indicating that the extra group had a remarkable influence on drug-protein interactions. However, many derivatives of CQ have not yet appeared, so we used molecular simulations to evaluate the effect of different groups on the binding capacity of CQ derivatives to SA. Since the hydrogen bond was the one of force in the interactions between CQ/HCQ and SA, on the basis of CQ (S1) and HCQ (S2), we selected -CHO (S3), -COOH (S4) and -NH_2 (S5), which were easy to form hydrogen bonds with amino acids as additional groups to study the effect of groups. As shown in Fig. S5 and Table S6, the introduction of hydrogen bond donor or acceptor groups, the scoring function of CQ derivatives and SA could be improved to a certain extent. When combined with BSA, -NH_3 (S5) group obtained the highest score after docking, while the structure containing -COOH (S4) groups had the highest score when combined with HSA, indicating that the hydrophilic groups might make CQ have stronger binding capacity with SA and less side effects, which should be further verified by experimental method.

4. Conclusion

In summary, to better elucidate the affinity interaction of COVID-19 drug candidates (CQ and HCQ) in the level of protein, a variety of techniques were used to study their interactions with BSA and HSA. The results showed that the intrinsic emission of both SA could be quenched by CQ and HCQ, and the quenching process were both spontaneous exothermic entropy reduction static process. The order of magnitude of binding constants were both in the second power of ten, and the binding capacity of the two drugs with BSA was greater than that with HSA, and the binding capacity to SA of HCQ was stronger than that of CQ. Differences in binding constants may be responsible for the efficacy and even for the different side effects. Binding site recognition demonstrated that CQ preferred to bind to the two sites of both SA, while HCQ tended to bind to the site I of SA. In the interactions between two drugs and SA, hydrogen bonds and van der Waals forces were the main force, which was verified by thermodynamic functions and molecular simulation. CQ and HCQ had weak effects on the structure of SA, which was mainly manifested in increasing the α-helix content of SA. The weak effects

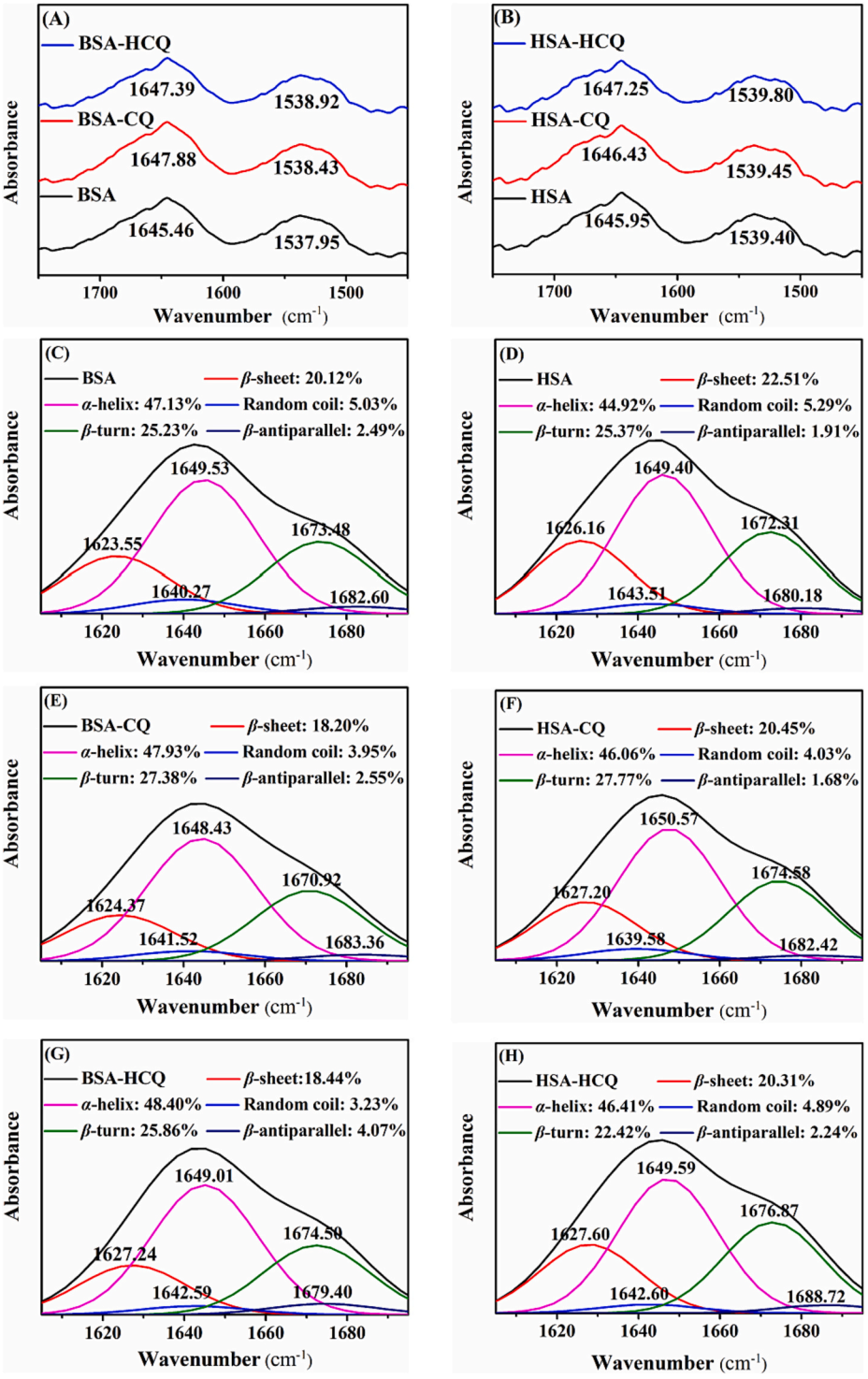

Fig. 6. FT-IR spectra of BSA (A) and HSA (B) in the absence and presence of CQ and HCQ; Fitting results of FT-IR spectra of BSA in the absence (C) and presence of CQ (E) and HCQ (G); Fitting results of FT-IR spectra of HSA in the absence (D) and presence of CQ (F) and HCQ (H). [SA] = [CQ] = [HCQ] = 500.00 μM.

could not cause side effects on the level of protein. The results of optimizing functional groups of CQ with molecular docking showed that the carboxylation and amination of CQ could make it bind strongly with SA and may have less side effects, which should be further verified by experimental method. We found that CQ/HCQ and its analogue 4-(4′-cyanophenoxy)-2-(4″-cyanophenyl)-aminoquinoline exhibited similar binding sites, binding forces and quenching mechanisms in the interaction with SA [48], indicating that the interaction between drugs and SA is largely influenced by the structure of the subject. This work provides guidance for functional group selection and drug efficacy improvement of chloroquine analogues.

CRediT authorship contribution statement

Lan-Yi Hu: Conceptualization, Investigation, Data curation, Writing – original draft, Visualization. **Ye Yuan:** Investigation, Validation. **Zi-Xuan Wen:** Investigation. **Yi-Yue Hu:** Investigation. **Miao-Miao Yin:** Methodology, Supervision, Writing – review & editing, Funding

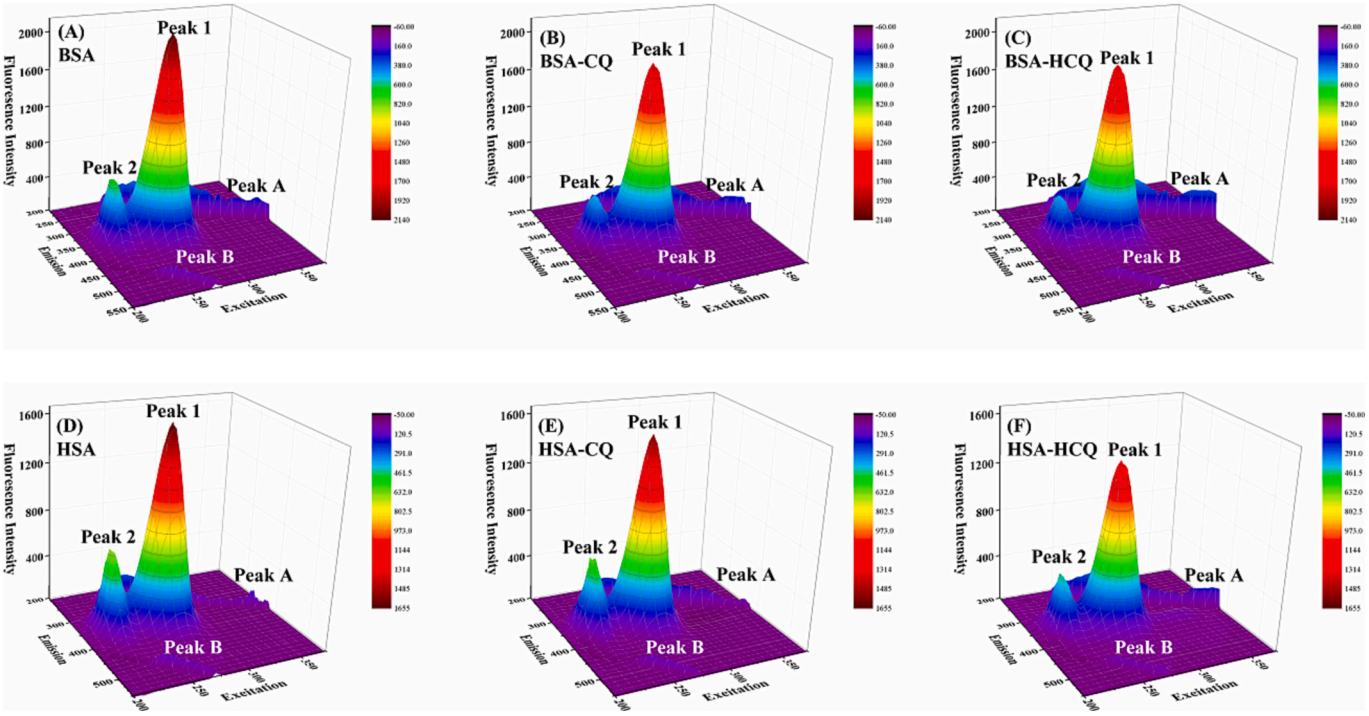

Fig. 7. 3D fluorescence spectra of BSA in the absence (A) and presence of CQ (B) and HCQ (C); 3D fluorescence spectra of HSA in the absence (D) and presence of CQ (E) and HCQ (F). [SA] = [CQ] = [HCQ] = 5.00 μM.

acquisition. **Yan-Jun Hu:** Conceptualization, Supervision, Funding acquisition, Project administration, Writing – review & editing, Funding acquisition.

Author statement

We agree to be accountable for all aspects of the work in ensuring that questions related to the accuracy or integrity of any part of the work are appropriately investigated and resolved.

The work reported in the manuscript has not been previously published in any language anywhere and that it is not under consideration for publication elsewhere. The work is approved by all authors and tacitly or explicitly by the responsible authorities where the work was carried out.

There are no interests to declare, and we please this state in the manuscript: 'Declarations of interest: none'.

Declaration of Competing Interest

The authors declare that they have no known competing financial interests or personal relationships that could have appeared to influence the work reported in this paper.

Data availability

No data was used for the research described in the article.

Acknowledgments

This work was supported by the National Natural Science Foundation of China (No. 22173029), Research Foundation of Education Bureau of Hubei Province, China (B2022157), Talent Introduction Project of Hubei Normal University (HS2021RC029).

Appendix A. Supplementary data

Supplementary data to this article can be found online at https://doi.org/10.1016/j.jphotobiol.2023.112667.

References

[1] C.L. Song, J. Qiao, S. Zhang, H.Y. Li, D.Y. Liu, Dose selection of chloroquine phosphate for treatment of COVID-19 based on a physiologically based pharmacokinetic model, Acta Pharm. Sin. B 10 (2020) 1216–1227.
[2] D.Z. Li, J.B. Hu, D. Li, W.J. Yang, S.F. Yin, R.H. Qiu, Reviews on biological activity, clinical trial and synthesis progress of small molecules for the treatment of COVID-19, Top. Curr. Chem. 379 (2021) 1–52.
[3] W.J. Huang, K.L. Wang, C.T. Huang, K.M. Chou, D. Tsang, R.W.M. Lai, R.H. Xu, E. K. Yeoh, C. Chen, K.F. Ho, Evaluation of SARS-CoV-2 transmission in COVID-19 isolation wards: on-site sampling and numerical analysis, J. Hazard. Mater. 436 (2022), 129152.
[4] Z. Xu, L. Shi, Y.J. Wang, J.Y. Zhang, C. Zhang, S.H. Liu, P. Zhao, H.X. Liu, L. Zhu, Pathological findings of COVID-19 associated with acute respiratory distress syndrome, Lancet Respir. Med. 8 (2020) 420–422.
[5] L.Z. Huang, Y.Q. Chen, J. Xiao, W.S. Luo, F. Li, Y. Wang, Progress in the research and development of anti-COVID-19 drugs, Front. Public Health 8 (2020) 365.
[6] M.L. Wang, R.Y. Cao, L.K. Zhang, X.L. Yang, J. Liu, M.Y. Xu, Z.L. Shi, Z.H. Hu, W. Zhong, G. Xiao, Remdesivir and chloroquine effectively inhibit the recently emerged novel coronavirus (2019-nCoV) in vitro, Cell Res. 30 (2020) 1–3.
[7] Z. Sahraei, M. Shabani, S. Shokouhi, A. Saffaei, Aminoquinolines against coronavirus disease 2019 (COVID-19): chloroquine or hydroxychloroquine, Int. J. Amtimicrob. Ag. 55 (2020), 105945.
[8] M. Bahadoram, B. Keikhaei, A. Saeedi-Boroujeni, M.R. Mahmoudian-Sani, Chloroquine/hydroxychloroquine: an inflammasome inhibitor in severe COVID-19? Pharmaco. 394 (2021) 997–1001.
[9] E. Keyaerts, L. Vijgen, P. Maes, J. Neyts, M. Van Ranst, In vitro inhibition of severe acute respiratory syndrome coronavirus by chloroquine, Biochem. Bioph. Res. Co. 323 (2004) 264–268.
[10] J.Y. Zhao, Y.X. Zhang, M.H. Wang, Q. Liu, X.B. Lei, M. Wu, S.S. Guo, D.R. Yi, Q. J. Li, L. Ma, Quinoline and Quinazoline Derivatives Inhibit Viral RNA Synthesis by SARS-CoV-2 RdRp 7, 2021, pp. 1535–4547.
[11] S.A. Mao, D.C. Klonoff, J. Akram, Efficacy of chloroquine and hydroxychloroquine in the treatment of COVID-19, Eur. Rev. Med. Pharmaco. 24 (2020) 4539–4547.
[12] T. Fiolet, A. Guihur, M.E. Rebeaud, M. Mulot, N. Peiffer-Smadja, Y. Mahamat-Saleh, Effect of hydroxychloroquine with or without azithromycin on the mortality of coronavirus disease 2019 (COVID-19) patients: a systematic review and meta-analysis, Clin. Microbiol. Infect. 27 (2021) 19–27.

[13] Z.M. Liao, Z.M. Zhang, L. Liu, Hydroxychloroquine/chloroquine and the risk of acute kidney injury in COVID-19 patients: a systematic review and meta-analysis, Ren. Fail. 44 (2022) 415–425.
[14] J.M. Sanders, M.L. Monogue, T.Z. Jodlowski, J.B. Cutrell, Pharmacologic treatments for coronavirus disease 2019 (COVID-19) a review, Jama J. Am. Med. Assoc. 323 (2020) 1824–1836.
[15] S. Gulletta, P. Della Bella, L. Pannone, G. Falasconi, L. Cianfanelli, S. Altizio, E. Cinel, V. Da Prat, A. Napolano, G. D'Angelo, L. Brugliera, E. Agricola, G. Landoni, M. Tresoldi, P.Q. Rovere, F. Ciceri, A. Zangrillo, P. Vergara, QTc interval prolongation, inflammation, and mortality in patients with COVID-19, J. Interv. Card. Electrophysiol. 63 (2022) 441–448.
[16] F.S. Sinkeler, F.A. Berger, H.J. Muntinga, M.M.P.M. Jansen, The risk of QTc-interval prolongation in COVID-19 patients treated with chloroquine, Neth. Hear. J. 28 (2020) 418–423.
[17] Y.J. Hu, Y. Lin, L.X. Zhang, R.M. Zhao, S.S. Qu, Studies of interaction between colchicine and bovine serum albumin by fluorescence quenching method, J. Mol. Struct. 750 (2005) 174–178.
[18] T.V. Acunha, O.A. Chaves, B.A. Iglesias, Fluorescent pyrene moiety in fluorinated C6F5-corroles increases the interaction with HSA and CT-DNA, J. Porphyrins Phthalocyanines 25 (2020) 75–94.
[19] Y.D. Livney, Milk proteins as vehicles for bioactives, Curr. Opin. Colloid. In. 15 (2010) 73–83.
[20] S. Hashemnia, F.K. Fard, Z. Mokhtari, A study of the interactions between ephedrine and human serum albumin based on spectroscopic, electrochemical and docking assessments, J. Mol. Liq. 348 (2022), 118058.
[21] A.R. Jalalvand, Chemometrics in investigation of small molecule-biomacromolecule interactions: a review, Int. J. Biol. Macromol. 181 (2021) 478–493.
[22] F. Nasiri, G. Dehghan, M. Shaghaghi, S. Datmalchi, M. Iranshahi, Probing the interaction between 7-geranyloxycoumarin and bovine serum albumin: spectroscopic analyzing and molecular docking study, Spectrohim. Acta. A 254 (2021), 119664.
[23] K. Phopin, W. Ruankham, S. Prachayasittikul, V. Prachayasittikul, T. Tantimongcolwat, Insight into the molecular interaction of cloxyquin (5-chloro-8-hydroxyquinoline) with bovine serum albumin: biophysical analysis and computational simulation, Int. J. Mol. Sci. 21 (2019) 249.
[24] X. Qi, D.X. Xu, J.J. Zhu, S.J. Wang, J.W. Peng, W. Gao, Y.P. Cao, Studying the interaction mechanism between bovine serum albumin and lutein dipalmitate: multi-spectroscopic and molecular docking techniques, Food Hydrocoll. 113 (2021), 106513.
[25] A. Shiekhzadeh, N. Sohrabi, M.E. Moghadam, M. Oftadeh, Kinetic and thermodynamic investigation of human serum albumin interaction with anticancer glycine derivative of platinum complex by using spectroscopic methods and molecular docking, Appl. Biochem. Biotechnol. 190 (2020) 506–528.
[26] F.D.S. Santos, C.H. de Silveira, F.S. Nunes, D.C. Ferreira, H.F.V. Victoria, K. Kranbrick, O.A. Chaves, F.S. Rodembusch, B.A. Iglesias, Photophysical, photodynamical, redox properties and BSA interactions of novel isomeric tetracationic peripheral palladium (II)-bipyridyl porphyrins, Dalton. T. 49 (2020) 16278–16295.
[27] L. Ding, Y.Y. Zhao, H.H. Li, Q.J. Zhang, W.T. Yang, B. Fu, Q.H. Pan, A highly selective ratiometric fluorescent probe for doxycycline based on the sensitization effect of bovine serum albumin, J. Hazard. Mater. 416 (2021), 125759.
[28] S.S. Zhang, R.X. Gan, L.S. Zhao, Q.M. Sun, H.Z. Xiang, X. Xiang, G. Zhao, H. Li, Unveiling the interaction mechanism of alogliptin benzoate with human serum albumin: insights from spectroscopy, microcalorimetry, and molecular docking and molecular dynamics analyses, Spectrohim. Acta. A 246 (2021), 119040.
[29] T.C. Liao, Y. Zhang, X.J. Huang, Z. Jiang, X. Tou, Multi-spectroscopic and molecular docking studies of human serum albumin interactions with sulfametoxydiazine and sulfamonomethoxine, Spectrohim. Acta. A 246 (2021), 119000.
[30] S. Rashtbari, G. Dehghan, Biodegradation of malachite green by a novel laccase-mimicking multicopper BSA-Cu complex: performance optimization, intermediates identification and artificial neural network modeling, J. Hazard. Mater. 406 (2021), 124340.
[31] L. Xu, H.T. Yang, R.X. Hu, Y.H. Liang, Y.C. Li, W.L. Xu, X.Y. Fan, Y.F. Liu, Comparing the interaction of four structurally similar coumarins from *fraxinus chinensis* roxb. With HSA through multi-spectroscopic and docking studies, J. Mol. Liq. 340 (2021), 117234.
[32] L.X. Gao, W.Q. Chen, Y. Liu, F.L. Jiang, Fluorescent labeling of human serum albumin by thiol-cyanimide addition and its application in the fluorescence quenching method for nanoparticle-protein interactions, Anal. Chem. 94 (2022) 3111–3119.
[33] S. Khashkhashi-Moghadam, S. Ezazi-Toroghi, M. Kamkar-Vatanparast, P. Jouyaeian, P. Mokaberi, H. Yazdyani, Z. Amiri-Tehranizadeh, M.R. Saberi, J. Chamani, Novel perspective into the interaction behavior study of the cyanidin with human serum albumin-holo transferrin complex: spectroscopic, calorimetric and molecular modeling approaches, J. Mol. Liq. 356 (2022), 119042.
[34] H.C. Ma, T. Zou, H. Li, H.M. Cheng, The interaction of sodium dodecyl sulfate with trypsin: multi-spectroscopic analysis, molecular docking, and molecular dynamics simulation, Int. J. Biol. Macromol. 162 (2020) 1546–1554.
[35] M. Dustkami, H. Mansouri-Torshizi, K. Abdi, E. Dehghanian, M. Saeidifar, F. Mohammadi, A couple of antitumor Pd(II) complexes make DNA-refolding and HSA-unfolding: experimental and docking studies, J. Mol. Liq. 349 (2022), 118450.
[36] M. Babayeva, Z. Loewy, Repurposing drugs for COVID-19: pharmacokinetics and pharmacogenomics of chloroquine and hydroxychloroquine, Pgarmacogen. Pers. Med. 13 (2020) 531–542.
[37] J.L. Gu, S.Y. Zheng, H. Zhao, T. Sun, Investigation on the interaction between triclosan and bovine serum albumin by spectroscopic methods, J. Environ. Sci. Health B 55 (2020) 52–59.
[38] S. Huang, H.M. Li, Y. Liu, L.Y. Yang, D. Wang, Q. Xiao, Investigations of conformational structure and enzymatic activity of trypsin after its binding interaction with graphene oxide, J. Hazard. Mater. 392 (2020), 122285.
[39] V.S. Camara, O.A. Chaves, B.B. de Araujo, P.F.B. Goncalves, B.A. Lglesias, Photoactive homomolecular bis(n)-Lophine dyads: multicomponent synthesis, photophysical properties, theoretical investigation, docking and interaction studies with biomacromolecules, J. Mol. Liq. 349 (2022), 118084.
[40] A. Aguilera-Garrido, T. Castillo-Santaella, F. Galisteo-Gonzalez, M.J. Galvez-Ruiz, J.A. Molina-Bolivar, J.A. Holgado-Terriza, M.A. Cabrerizo-Vilchez, J. Maldonado-Valderrama, Applications of serum albumins in delivery systems: differences in interfacial behaviour and interacting abilities with polysaccharides, Adv. Colloid. Interfac. 209 (2021), 102365.
[41] J.L. Liu, Y.L. He, D. Liu, Y. He, Z.P. Tang, H. Lou, Y.P. Huo, X.Y. Cao, Characterizing the binding interaction of astilbin with bovine serum albumin: a spectroscopic study in combination with molecular docking technology, RSC Adv. 8 (2018) 7280–7286.
[42] I. Singh, V. Luxami, K. Paul, Spectroscopy and molecular docking approach for investigation on the binding of nocodazole to human serum albumin, Spectrohim. Acta. A 235 (2022), 118289.
[43] F. Yazdani, B. Shareghi, S. Farhadian, L. Momeni, Structural insights into the binding behavior of flavonoids naringenin with human serum albumin, J. Mol. Liq. 349 (2022), 118431.
[44] B.L. Wang, D.Q. Pan, S.B. Kou, Z.Y. Lin, J.H. Shi, Exploring the binding interaction between bovine serum albumin and perindopril as well as influence of metal ions using multi-spectroscopic, molecular docking and DFT calculation, Chem. Phys. 530 (2020), 117234.
[45] B.L. Sun, P.Q. Yu, Revealed interactive association between macro-molecular structures and true nutrition supply in cool-season adapted CDC chickpeas and CDC barley using advanced vibrational molecular spectroscopic techniques, J. Food Compos. Anal. 115 (2023), 104857.
[46] S.B. Yang, Q.L. Zhang, H.Y. Yang, H.M. Shi, A.C. Dong, L. Wang, S.N. Yu, Progress in infrared spectroscopy as an efficient tool for predicting protein secondary structure, Int. J. Biol. Macromol. 206 (2022) 175–187.
[47] L. Xu, H.T. Yang, R.X. Hu, Y.H. Liang, Y.C. Li, W.L. Xu, X.Y. Fan, Y.F. Liu, Comparing the interaction of four structurally similar coumarins from *Fraxinus Chinensis* Roxb. with HSA through multi-spectroscopic and docking studies, J. Mol. Liq. 340 (2021), 118084.
[48] S. Patnin, A. Makarasen, M. Kuno, S. Deeyohe, S. Techasakul, A. Chaivisuthangkura, Binding interaction of potent HIV-1 NNRTIs, amino-oxydiarylquinoline with the transport protein using spectroscopic and molecular docking, Spectrohim. Acta. A 233 (2020), 118159.